

Aging of a nanostructured $\text{Zn}_{50}\text{Se}_{50}$ alloy produced by mechanical alloying

K. D. Machado*, J. C. de Lima, C. E. M. de Campos,
T. A. Grandi, A. A. M. Gasperini

*Depto de Física, Universidade Federal de Santa Catarina, Trindade, Cx. P. 476,
88040-900, Florianópolis, Santa Catarina, Brazil*

Abstract

The aging at room temperature of a nanocrystalline equiatomic ZnSe alloy produced by mechanical alloying was investigated using X-ray diffraction (XRD) and differential scanning calorimetry (DSC) techniques. The measured XRD patterns showed the presence of the peaks corresponding to the crystalline trigonal selenium (*c*-Se) phase. It is observed that the ZnSe phase is stable with aging. The arising of the *c*-Se phase is attributed to the migration of Se atoms located at the interfacial component of the as-milled ZnSe nanostructure with aging.

Key words: Mechanical alloying, x-ray diffraction, semiconductors.

PACS: 61.10.-i, 81.70.P

1 Introduction

Due to their physical and chemical characteristics, selenium-based alloys are very important from technological and scientific points of view, mainly those alloys containing germanium or zinc because of their very interesting optical properties. For example, zinc selenide (ZnSe) is used in infrared lenses field. More recently, researches on semiconductor quantum dots have shown that it can also be used in short-wavelength visible-light laser devices [1]. According to them, the use of ZnSe in this field needs that the alloy is synthesized in nanometer form, with crystallite sizes smaller than the ZnSe exciton Bohr diameter ($\approx 90 \text{ \AA}$). For this purpose, techniques such as arrested nucleation in

* Corresponding author.

Email address: kleber@fisica.ufsc.br (K. D. Machado).

glasses, precipitation from sol-gel solutions and entrapment in porous sites inside zeolite cavities have been employed. These techniques, beyond expensive, are not able to full control the size of the nanoparticles obtained.

Mechanical alloying (MA) [2] has been used for almost two decades to produce many unique materials. These include, for instance, nanostructured alloys, amorphous compounds and unstable and metastable phases [1,3,4,5,6,7,8,9]. This method has several intrinsic advantages, like low temperature processing, easy control of composition, relatively inexpensive equipment, and the possibility of scaling up. Although the MA technique is relatively simple, the physical mechanisms involved are not yet fully understood. In order to make use of this technique in industrial applications, a better understanding of these physical mechanisms is desirable.

From a structural point of view, nanostructured materials can be regarded as being made of two components, one crystalline, with dimensions of the order of some nanometers, that preserves the structure of bulk crystal, and one interfacial, composed by defect centers. This component has caused controversy in the literature. Gleiter [10] has described it based on a gaseous model while other authors [11] disagree. The number of atoms in both components is similar [12]. Due to this fact, nanostructured material properties are strongly dependent of the interfacial component. From a technological point of view, manipulation of the interfacial component makes it possible to design materials with desired physical properties for specific applications [12,13].

The Zn-Se phase diagram [14] shows only an equiatomic ZnSe phase. In a recent paper [15] de Lima *et al.* reported structural results obtained from the application of MA to $\text{Zn}_{1-x}\text{Se}_x$ ($x = 0.20, 0.30, 0.40, 0.50, 0.70$ at. %) mixtures. The measured X-ray diffraction (XRD) patterns for the mixtures with nominal compositions different of the equiatomic one showed the peaks associated to the ZnSe phase and those ones associated to the majority component. In the case of Se-rich mixtures, Se excess was found in amorphous state. More recently, in other paper [16], de Lima *et al.* reported results on the influence of aging in the structural properties of the amorphous selenium (α -Se) produced by ball milling (BM). They have observed that the atomic structure of α -Se produced by BM, which is formed by Se_n chains, has transformed partially to another known α -Se structure formed by Se_8 rings found in the amorphous state obtained by rapid quenching or vapor deposition methods. Based on this interesting observation, an aged nanostructured ZnSe sample produced by MA some years ago was re-examined by using XRD and DSC techniques. To our knowledge, it is the first time that such study is reported.

2 Experimental procedure

A nanostructured equiatomic ZnSe sample (hereafter called ZnSe-97) was prepared by MA in 1997 following the procedure described in Ref. [15]. The X-ray diffraction (XRD) pattern measured after milling was indexed to the cubic zinc selenide phase (isostructural with the structure of ZnS compound), with lattice parameter $a = 5.6478 \text{ \AA}$. After four years being kept in a dry desiccator a new XRD pattern of the same sample (hereafter called aged-ZnSe-97) was measured in order to verify possible structural changes. The comparison between the XRD patterns of the as-milled and aged samples shows significant differences that will be discussed later. To ensure reproducibility of the ZnSe-97, a new equiatomic ZnSe sample was prepared by MA. Its XRD pattern was identical to that recorded for the as-milled ZnSe-97 sample.

Small quantities of the aged-ZnSe-97 sample were heat treated at 196°C and 350°C in quartz capsules containing argon. Only the sample heated at 350°C was quenched. The other was air-cooled. During the heat treatment at 350°C , formation of water drops at the inner walls of the capsule was observed, indicating that the samples are hydrophilic. All heated samples were analyzed using a Rigaku powder diffractometer, Miniflex model, with Cu K_α radiation ($\lambda = 1.5418 \text{ \AA}$) and a TA 2010 Differential Scanning Calorimetry (DSC) cell with a heating rate of $10^\circ\text{C}/\text{min}$ in a flowing argon atmosphere.

3 Results and discussion

The measured XRD patterns for ZnSe-97, aged-ZnSe-97 and crystalline selenium in its trigonal form (*c*-Se) are shown in Figs. 1.a, 1.b and 1.c, respectively. In a previous study [15] we showed that the XRD pattern seen in Fig. 1.a corresponds to the nanostructured ZnSe compound. A comparison between Figs. 1.a and 1.b shows that this phase is also seen in the aged-ZnSe-97 sample. This indicates that the ZnSe phase is as stable with aging as expected. In addition to the peaks associated with the ZnSe phase, Fig. 1.b displays several other peaks that were indexed to the *c*-Se phase and that are absent in Fig. 1.a. The remaining low intensity peaks seen in Figs. 1.a and 1.b were indexed to a contaminant ZnO phase according to the JCPDS card No. 1-1136 [17]. Their low intensities when compared to those associated with the ZnSe phase suggested that this contaminant should be found in a small quantity, and a Rietveld analysis [18] (discussed below) confirmed this assumption.

The ZnSe-97 and aged-ZnSe-97 patterns shown in Figs. 1.a and 1.b were simulated using the Rietveld procedure [18] considering ZnSe, *c*-Se and ZnO phases. The results obtained show that the lattice parameter of the ZnSe

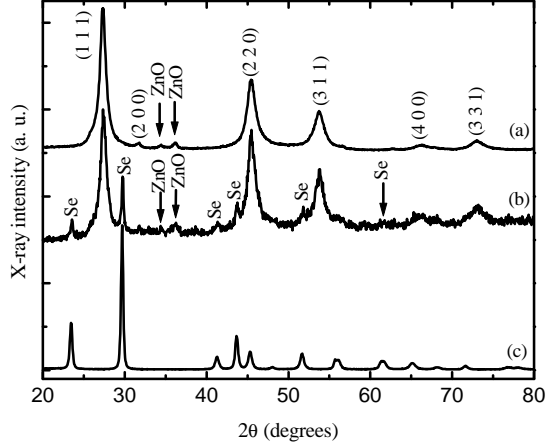


Fig. 1. XRD patterns for (a) ZnSe-97, (b) aged-ZnSe-97 and (c) crystalline Se phase.

phase changes with aging within 0.1% and their values are listed in Table 1. Besides that, about 93% of the crystalline phases are given by the ZnSe phase and 7% by the ZnO phase in the as-milled sample, whereas in the aged sample the ZnSe, ZnO and *c*-Se phases are responsible for about 73%, 16% and 11% of the phases, respectively (see Fig. 2). By using the full width of half maximum (FWHM) obtained from the simulated patterns and the Scherrer formula [19] the average crystallite sizes of the phases were estimated. The results for the ZnSe phase are found in Table 1. Its value for the ZnO phase is 129 Å in the as-milled and 135 Å in the aged samples. In the aged sample, the *c*-Se phase has an average crystallite size of 335 Å, indicating that all phases are found in the nanometric form. As mentioned above, nanostructured alloys are described by two components, one crystalline and other interfacial. Thus, the segregation of the *c*-Se particles in the aged sample could have had its origin in the migration of Se atoms located at the interfacial component and, if this is true, it is a remarkable fact since the *c*-Se segregation process has occurred at room temperature. According to Gleiter [10], the interfacial component is formed by a high density of interfaces ($\approx 10^{19} \text{ cm}^{-3}$), which gives rise to a high density of short diffusion paths. As a consequence of the presence of an interfacial component in the nanostructured material, it is expected an increase in the diffusion coefficient in comparison with single crystals and polycrystals with the same chemical composition. For instance, according to Birringer *et al.* [20], the self-diffusivity in nanocrystalline copper (80 Å) at 353 K is $10^{-18} \text{ m}^2/\text{s}$ while in the lattice its value is $10^{-34} \text{ m}^2/\text{s}$. Partial amorphous structural transformation with aging at room temperature had also been observed in amorphous selenium produced by BM [16].

To investigate the presence of residual non-reacted Se in the ZnSe-97 sample, which could have not been detected by the XRD measurement, a DSC measurement was performed and it is shown in Fig. 3.a. It displays three endothermic peaks located at 75°C, 200°C and 310°C. These peaks, except that

Table 1

Lattice parameters and average crystallite sizes of ZnSe phase prepared by MA.

Sample	Lattice parameter (Å)	Average crystallite size (Å)
ZnSe-97	5.6478	96
aged-ZnSe-97	5.6408	92
aged-ZnSe-97 (treat. at 196°C)	5.6443	107
aged-ZnSe-97 (treat. at 350°C)	5.6578	189
JCPDS card. No. 37-1463	5.6688	—

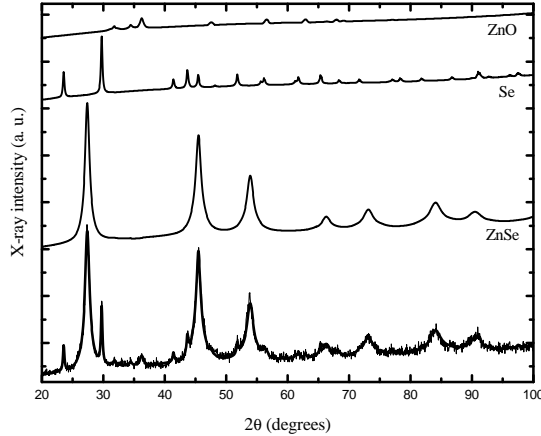


Fig. 2. XRD pattern of the aged-ZnSe-97 (bottom) and its Rietveld fitting (thick line) using ZnSe, *c*-Se and ZnO phases.

at 200°C, were associated with water, as will be discussed later. The peak at 200°C is associated with the melting of a very small quantity of *c*-Se phase. These *c*-Se particles could have acted as “seeds” for the growing of the *c*-Se phase identified in the aged-ZnSe-97 (see Fig. 1.b). Fig. 3.b, which corresponds to the DSC curve of the aged-ZnSe-97 sample, shows three endothermic peaks located at 100°C, 200°C and 300°C. As it happened to the ZnSe-97 sample, the peaks at 100°C and 300°C were associated with water. The peak at 200°C in this figure is higher than that in Fig. 3.a suggesting the growing of the *c*-Se phase, in agreement with the XRD results.

To determine the origin of the peaks located around 75–100°C and 300°C in the DSC measurements of ZnSe-97 and aged-ZnSe-97 (see Figs. 3.a and 3.b) we performed a heat treatment in a small quantity of the aged-ZnSe-97 sample at 350°C followed by a quenching in iced water. After it was made we noted the formation of water drops at the inner walls of the capsule, indicating that the sample was hydrophilic. The DSC measurement of the quenched sample shown in Fig. 3.c confirmed this assumption since in this curve the peaks located around 75–100°C and 300°C were not seen anymore. These peaks can be explained by the release and vaporization of adsorbed water at the surface

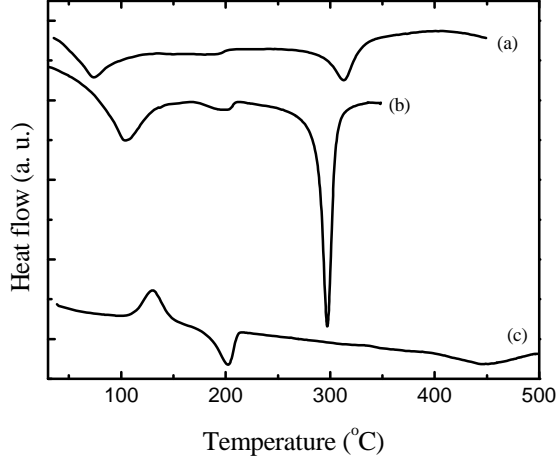


Fig. 3. DSC spectra for (a) ZnSe-97, (b) aged-ZnSe-97 and (c) aged-ZnSe-97 after heat treatment at 350°C.

and inside of the crystallites, respectively. The increase in the intensity of the peaks in the aged-ZnSe-97 DSC spectrum is due to the quantity of water adsorbed during aging. The exothermic peak about 130°C and the endothermic one at 200°C (see Fig. 3.c) are associated with the amorphous-crystalline Se transformation and with the melting of the *c*-Se formed, respectively.

In order to investigate the influence of the temperature in the growing of the *c*-Se phase observed in the aged-ZnSe-97 sample, another small quantity of the aged-ZnSe-97 sample was heat treated at 196°C. At this temperature water was not observed at the inner walls of the capsule, indicating that almost all water observed in the sample quenched at 350°C was released from inside the crystallites. The measured XRD pattern of the sample heat treated at 196°C is shown in Fig. 4.a. Its comparison with that of the aged-ZnSe-97 sample displayed in Fig. 1.b reveals that this heat treatment has only caused a slight improvement in the crystallinity of the ZnSe phase, as it can be seen by comparing the lattice parameters and average crystallite size values given in Table 1. The Rietveld analysis indicates that there is no change in the phase quantities with the heat treatment, therefore suggesting that the alloy had already reached its thermodynamic stability before the heat treatment. The crystallinity of the ZnSe phase is significantly improved only at 350°C, as indicated by its XRD pattern (see Fig. 4.b) and by its lattice parameter given in Table 1. As expected, the XRD pattern of the quenched sample does not show the peaks associated with *c*-Se anymore, in agreement with the DSC measurement (see Fig. 3.c), which shows that the Se particles are found in an amorphous phase. In addition, Rietveld analysis indicates that the ZnSe and ZnO phases correspond to about 84% and 16% of the crystalline phases found in this sample, respectively. These data indicate an increase in the quantity of the ZnO phase as compared to that in the ZnSe-97 sample. The average crystallite size of the ZnO phase also increases, reaching 268 Å.

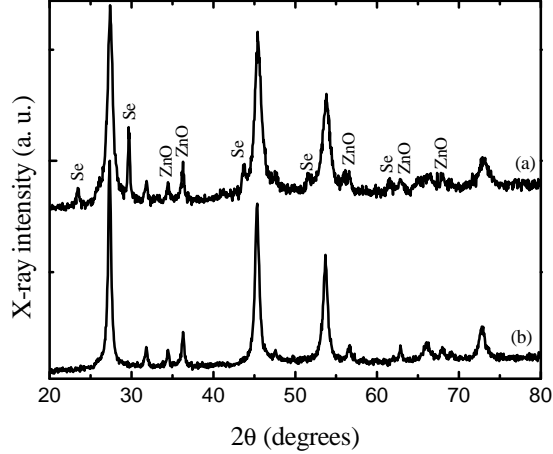


Fig. 4. XRD patterns for aged-ZnSe-97 heat treated at (a) 196°C and (b) 350°C.

4 Conclusion

The influence of aging in a nanocrystalline equiatomic ZnSe alloy prepared by MA was investigated. Based on the results found, we conclude that:

- (1) The nanocrystalline equiatomic ZnSe alloy produced by MA is as stable as those prepared by using other methods (melting, for instance), as indicated by the XRD patterns seen in Figs. 1 and 4.
- (2) Due to the presence of a small quantity of *c*-Se phase in the as-milled sample and to the properties of the interfacial region already described in the text, the room temperature energy (≈ 0.025 eV) is sufficient to promote migration of Se atoms located at this component. This fact causes growing of the *c*-Se phase, as it could be seen in the aged-ZnSe-97 XRD pattern (Fig. 1.b).
- (3) After four years the growing of the *c*-Se phase has finished, and the crystalline phases in the sample have reached their thermodynamic stability, as indicated by the XRD measurements and Rietveld analyses of the aged- and heat-treated at 196°C ZnSe-97 samples (Figs. 1.b and 4.a).
- (4) The samples are hydrophilic, as indicated by the DSC measurements shown in Fig. 3.

Acknowledgements

We thank to the Brazilian agencies CNPq, CAPES and FINEP for financial support.

References

- [1] V. J. Leppert, S. Mahamuni, N. R. Kumbhojkar, S. H. Risbud, *Mater. Sci. Eng. B52* (1989) 89.
- [2] C. Suryanarayana, *Prog. Mater. Sci.* 46 (2001) 1.
- [3] J. C. de Lima, E. C. Borba, C. Paduani, V. H. F. dos Santos, T. A. Grandi, H. R. Rechenberg, I. Denicoló, M. Elmassalami, A. P. Barbosa, *J. Alloys Comp.* 234 (1996) 43.
- [4] A. W. Weeber, H. Bakker, *Physica B* 153 (1988) 93.
- [5] D. K. Mukhopadhyay, C. Suryanarayana, F. H. Froes, *Scripta Metall. Mater.* 30 (1994) 133.
- [6] A. R. Yavari, P. J. Desré, T. Benameur, *Phys. Rev. Lett.* 68 (1992) 2235.
- [7] C. E. M. Campos, J. C. de Lima, T. A. Grandi, K. D. Machado, P. S. Pizani, *Sol. State. Commun.* 123 (2002) 179.
- [8] C. E. M. Campos, J. C. de Lima, T. A. Grandi, K. D. Machado, P. S. Pizani, *Physica B* 324 (2002) 409.
- [9] K. D. Machado, J. C. de Lima, C. E. M. de Campos, T. A. Grandi, D. M. Trichês, *Phys. Rev. B* 66 (2002) 94205.
- [10] H. Gleiter, *Nanostruct. Mater.* 1 (1992) 1.
- [11] E. A. Stern, R. W. Siegel, M. Newville, P. G. Sanders, D. Haskel, *Phys. Rev. Lett.* 75 (1995) 3874.
- [12] T. Grandi, V. H. F. dos Santos, J. C. de Lima, *Solid State Commun.* 112 (1999) 359.
- [13] T. Grandi, V. H. F. dos Santos, J. C. de Lima, *Solid State Commun.* 110 (1999) 673.
- [14] M. Hansen, K. Anderko, *Constitution of Binary Alloys*, 2nd Edition, Genium Publishing Corp./McGraw-Hill, New York, 1991.
- [15] J. C. de Lima, V. H. F. dos Santos, T. A. Grandi, *Nanostruct. Materials* 11 (1999) 51.
- [16] J. C. de Lima, T. A. Grandi, R. S. de Biasi, *J. Non-Cryst. Solids* 286 (2001) 93.
- [17] JCPDS - Powder Diffraction File Search Manual (International Center for Diffraction Data, Pennsylvania, U.S.A., 1996).
- [18] H. M. Rietveld, *J. Appl. Crystallogr.* 2 (1965) 65.
- [19] H. P. Klug, L. E. Alexander, *X-Ray Diffraction Procedures for Polycrystalline and Amorphous Materials*, 2nd Edition, John Wiley & Sons, New York, 1974.
- [20] R. Birringer, H. Hahn, H. Höfler, J. Karch, H. Gleiter, *Defect and Diffusion Forum* 59 (1988) 17.